# Effect of Wind Speed on Mixing Region Aerosol Concentrations at a Tropical Coastal Station

K. PARAMESWARAN, G. VIJAYAKUMAR, B. V. KRISHNA MURTHY, AND K. KRISHNA MOORTHY

*Space Physics Laboratory, Vikram Sarabhai Space Centre, Thiruvananthapuram, India*

(Manuscript received 11 August 1994, in final form 21 November 1994)

ABSTRACT

Altitude distribution of aerosols in the mixing region in a tropical coastal environment is studied using a bistatic continuous-wave lidar. It is found that aerosols remain fairly well mixed—their number density showing little variation with altitude up to an altitude of approximately 300 m from the surface, and above this their number density, in general, decreases with an increase in altitude. The aerosol number density shows a significant dependence on the near-surface wind speed. This dependence could be represented fairly well by an exponential function of wind speed. The wind contribution to aerosol content is found to be at its maximum during the southwest monsoon period.

## 1. Introduction

Atmospheric aerosols are produced by a variety of processes. These include direct injection of particles due to windblown dust and soil erosion due to wind. Also, in marine and coastal regions, sea-spray aerosols due to surface winds play an important role. Other important production processes include gas-to-particle conversion and industrial effluvia. The aerosol loss processes are the wet removal and gravitational sedimentation. Transport plays an important role in the distribution of atmospheric aerosols. A study of atmospheric aerosols in relation to their dependence on meteorological parameters will help in understanding the role of these in the aerosol distribution, especially in the boundary layer. While such studies have been carried out at high-latitude stations (Fernald et al. 1972; Sasano 1985; Kim et al. 1988; Suzuki and Tsunogai 1988; Hoppel et al. 1990; Park et al. 1990), there is a relative paucity at tropical regions. In view of the different meteorological conditions prevailing over the Tropics, including the monsoon system in the southeast Asian region, such studies would be of great interest. In this paper we report the results of a study on the influence of meteorological parameters such as wind speed and rainfall on aerosols in the mixing region at the coastal station, Trivandrum (8°33'N, 77°E). This station is located on the southwest coast of India and is subject to both the southwest and northeast monsoons during the months of June–November.

*Corresponding author address:* Dr. B. V. K. Murthy, Space Physics Laboratory, Vikram Sarabhai Space Centre, Trivandrum 695 022, India.

## 2. Experimental setup

Altitude profiles of aerosol number density are obtained up to an altitude of approximately 1100 m using a continuous-wave (CW) lidar system operated in bistatic mode. Details of the lidar system and method of deducing altitude profiles of aerosol number density from the lidar observations have been presented earlier by Parameswaran et al. (1984). The lidar system essentially consists of an $Ar^+$ laser operated at 500 mW of optical power at 514.5 nm with a beamwidth of $0.28 \times 10^{-6}$ sr and a transmission-type telescope with an effective collecting area of 0.07 $m^2$ to receive the scattered signal. The transmitter and receiver are horizontally separated by a distance of 380 m. The laser beam is linearly polarized and configured such that the electric vector is along the scattering plane. The lidar has been used to measure the angularly scattered signal strength from different altitudes in the range of 50–1100 m by suitably orienting the receiving telescope and keeping the transmitted beam in the vertical. Regular observations have been carried out around 2000 IST on days with clear sky conditions. From these measurements, the altitude profiles of aerosol number density $N_a$ are obtained using the Mie scattering cross section of aerosols after accounting for the molecular scattering. In obtaining these profiles, it is assumed that the aerosol size distribution is of modified power-law type (McClatchey et al. 1972) with size index 4.5 and an effective aerosol refractive index 1.45, which is generally true for the mixing region aerosols over this station (Parameswaran and Vijayakumar 1993). The $N_a$ profiles in each month are averaged to obtain representative monthly mean profiles.

## 3. Results and discussion

From the monthly mean $N_a(h)$ profiles from 50 m to 1.1 km obtained from these observations, the aerosol optical depth $\tau_a$ up to 1.1 km is obtained assuming that the aerosol number density remains the same from ground to a 50-m altitude. The month-to-month variation of $\tau_a$ is presented in Fig. 1 along with the respective averages of the relevant meteorological parameters, namely, the wind speed ($U$) and the surface relative humidity (RH) and the monthly total rainfall (RF). The mean wind speed $\bar{U}$ at 1500 IST is obtained from the meteorological observations approximately 10 m above mean sea level (MSL) at the Trivandrum airport, situated close to the lidar site, and is the average for the days of lidar observation. The wind measurement site and lidar observation site are located almost at the same distance from the seacoast ($\sim$500 m). The lidar observation site is about 3 m MSL, and all altitudes referred in this paper correspond to those above the MSL. The mean surface RH for each month is obtained by averaging the surface relative humidity values measured using a hygrometer at the lidar site during the observation period.

In the estimation of aerosol number densities (and hence $\tau_a$) from the lidar signal, we have used a fixed combination of size index (4.5) and refractive index (1.45). But as the atmospheric relative humidity increases, more water vapor from the atmosphere condenses on to the aerosol particles resulting in their growth (Hanel 1976). This causes a decrease in size index. The decrease in size index would result in an increase in the effective Mie scattering cross section if the particle refractive index remains the same. Then usage of a fixed size index (which may be greater than the actual) would lead to an overestimate of $N_a$. But, as the relative humidity increases, the refractive index of the particle decreases (Shettle and Fenn 1979). This causes a reduction in the effective Mie scattering cross section, if the size index remains the same. Decrease in cross section causes an increase in the estimated values of $N_a$. Then usage of a fixed refractive index (which is more than the actual) would lead to an underestimate of $N_a$. But in the actual situation, the refractive index and size index vary simultaneously, both decreasing with an increase in relative humidity. The decrease in size index causes an increase in the Mie scattering cross section, whereas the decrease in refractive index causes a decrease in the Mie scattering cross section. Thus, these two aerosol parameters have opposite effects on the scattering cross section. On examining this aspect further, by using Hanel's "model 6" (Hanel 1976) and maritime model of aerosol refractive index by Shettle and Fenn (1979), it is found that the range of variation in aerosol scattering cross section is approximately 35% as RH varies from 0% to 85%. The variation of scattering cross section is insignificant for RH < 60%. Considering the seasonal

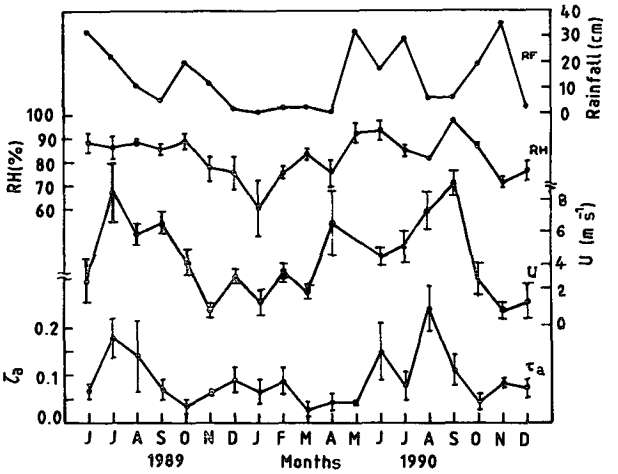


FIG. 1. Seasonal variation of aerosol optical depth ($\tau_a$) in the altitude region 0–1.1 km, along with that of mean wind speed ($\bar{U}$), surface relative humidity (RH), and monthly total rainfall (RF).

variation of RH in Fig. 1, it can be seen that the mean RH for monsoon months (June–November) is 85% $\pm$ 6% and for the nonmonsoon months it is 75% $\pm$ 9%. For this range of variation in RH, the Mie scattering cross section varies by 30%. Thus, changes in seasonal variation of RH can cause an uncertainty of about $\pm$15% in the derived $N_a$ profiles through the variations in the size index and the aerosol refractive index. The altitude variation of RH in the first 1 km is generally less than 5% and is still smaller during the monsoon months (Parameswaran 1988). As the aerosols in the first 1 km generally remain fairly mixed, and the altitude variation of RH is rather small, the effect of change in size distribution with altitude will be negligible. Thus, the uncertainty in $N_a$ due to the assumption of a fixed size distribution of aerosols in this region can be taken to be within $\pm$15%.

Being situated at the coast, this station is subjected to the sea-breeze activity on all the days. The sea breeze generally sets in around 0900 IST in the morning (Prakash 1993; Prakash et al. 1993). Soon after the onset, the sea breeze strengthens and continues throughout up to 2–3 h after the local sunset. The wind speed is maximum around 1500 IST and then decreases slowly with time (Nair et al. 1993). The wind direction changes to seaward only in the late night hours. Thus, throughout the day and for a few hours after the sunset, during which the lidar observations are done, sea-breeze activity prevails over this coast. The mean wind speed $\bar{U}$ shown in Fig. 1 is taken to represent the sea-breeze activity.

The aerosol optical depth $\tau_a$ shows (Fig. 1) prominent maxima during the southwest monsoon months of June–September (1989 and 90) and a weak secondary maximum during the winter months of November–February. The aerosol optical depth is minimum in March and October months. Figure 1 also shows that

there is a good correspondence between $\bar{U}$ and $\tau_a$, with $\tau_a$ being higher in months in which $\bar{U}$ is high and vice versa. Surface relative humidity is high during the monsoon period and low during the winter months (December–February). The same is true for the monthly total rainfall also. No significant correspondence is observed between $\tau_a$ and these two (RH and RF) meteorological factors. To quantify the dependence of $\tau_a$ on these meteorological parameters, the correlation coefficients were evaluated. The value of the correlation coefficient between $\tau_a$ and $\bar{U}$ is 0.59, that between $\tau_a$ and RH is 0.29, and that between $\tau_a$ and RF is close to 0. From the above, it can be seen that there exists a significant correlation between $\tau_a$ and $\bar{U}$. The correlation of $\tau_a$ with the other two parameters is not significant.

In the first week of June, the southwest monsoon sets in over the Arabian seacoast. The strong southwesterly monsoon winds blowing from the sea agitate the sea surface, resulting in the production of sea-spray aerosols, advection of which onto the coast causes an increase of the aerosol content in the coastal mixing region (resulting in an increase in $\tau_a$). The relation between the wind speed and marine aerosols has been demonstrated by many investigators (Monahan et al. 1983; Toba 1961) by direct sampling of aerosol particles in a marine environment. They observed an increase in the aerosol concentration with increasing wind speeds. The southwest monsoon winds also bring abundant moisture over this continent causing an increased rainfall (Fig. 1). This increased rainfall also increases the wet-removal rate causing a depletion of the mixing region aerosol content. So, one would expect a decrease in $\tau_a$ with an increase in rainfall, which is not observed in Fig. 1. The wet-removal process consists of two parts, namely rainout (incorporation of particles in precipitation droplets during processes occurring within the cloud) and washout (incorporation of material into precipitation as a consequence of processes occurring below the cloud base). Flossmann et al. (1985) modeled the wet removal of aerosol particles and found that the nucleation scavenging (the former) is mainly confined to aerosol particles larger than 0.1 $\mu$m in radius. Theoretical modeling of precipitation scavenging (washout) for polydisperse aerosols (Hidy 1984) shows that the collision efficiency is large for both large and small particles with a minimum at the intermediate sizes in the 0.2–0.5 $\mu$m (Greenfield gap). As the present study is concerned with altitudes below 1 km, which is below the general cloud-base height over this station (Rao 1976) during the monsoon season, nucleation scavenging can be expected to be less effective. The dominant wet-removal process of interest then is the precipitation scavenging, which is relatively weak (Radke et al. 1980) for particles in the radius range of 0.2–0.5 $\mu$m (compared to the remaining portion of the size spectrum), sensitive to scattering at the wavelength of operation of the lidar. Also, the lidar observations during the monsoon months are conducted during its "break" period such that rainfall is scanty at least 2 days prior to observation. Also, any depletion of aerosol particles by washout would be replenished at least partially due to the increased production due to wind, considering a residence time of approximately 1 day for this altitude region (Jaenicke 1980). Thus, the observed increase in $\tau_a$ during the monsoon months can be attributed to the increased aerosol production by wind overriding the wet-removal process.

## 4. Dependence of aerosol number density on wind speed

Governed by different production and loss mechanisms, the aerosol particles in the atmosphere will have a definite residence time (Jaenicke 1984). This residence time varies with aerosol size and altitude at which they are located. Very small particles ($r < 0.01$ $\mu$m) are lost by coagulation more rapidly than intermediate size particles. The large (or giant) particles are removed fast by the gravitational sedimentation. Those particles in the intermediate-size range (0.1–5 $\mu$m) will have a reasonably large residence time (Jaenicke 1984). As significant contribution to scattering at the lidar wavelength (514.5 nm) comes from this size range, the aerosol number density (or optical depth) discussed in the present context pertains to these long-lived particles. The residence time of such aerosol particles estimated (Pruppacher and Klett 1978) from different model parameters for altitudes below 1.5 km is 0.5–1 day. So the altitude profiles of aerosol number density observed by the lidar at about 2000 IST are a result of accumulation from earlier hours. Also, the mixing region aerosols dispersed by the convective motion during the daytime remain there even after the sunset for about 4–6 h (Delage 1974). Thus, the effect of wind speed on mixing region aerosol number density is rather complex, and the effect of local wind and wind speed history are strongly coupled (Gathman 1983).

As a first step to quantify the wind speed dependence, we have examined the correlation between the aerosol number density at different altitudes in the range of 0–1.1 km. Altitude profiles of aerosol number density obtained on different days during the period 1989–90 and the wind speed $U$ recorded at 1500 IST on that day have been used for this purpose. About 70 daily profiles of $N_a$ in this period have been employed. Being situated on the Arabian seacoast, in the southern tip of the Indian Peninsula, this station experiences sea breeze throughout the daytime, as well as for a few hours after the sunset, all through the year. The coastline is along the 325°–145° azimuth (0° referring to geographic north as per the standard convention), and during the daytime the wind direction always lies in the range of 200°–300° (i.e., blowing from the sea). Thus, irrespective of the season, wind contribution to

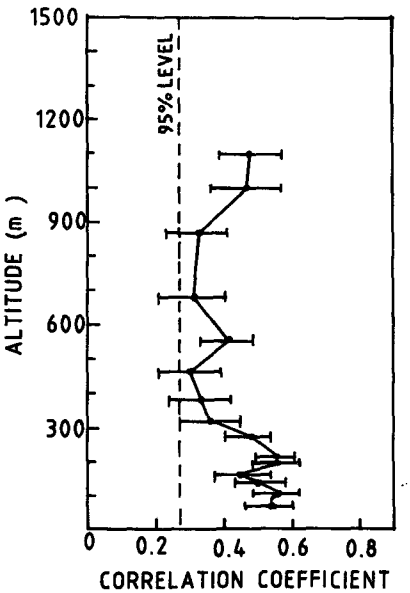


FIG. 2. Altitude variation of the correlation coefficient between aerosol number density and wind speed. The horizontal lines represent the error in the associated correlations.

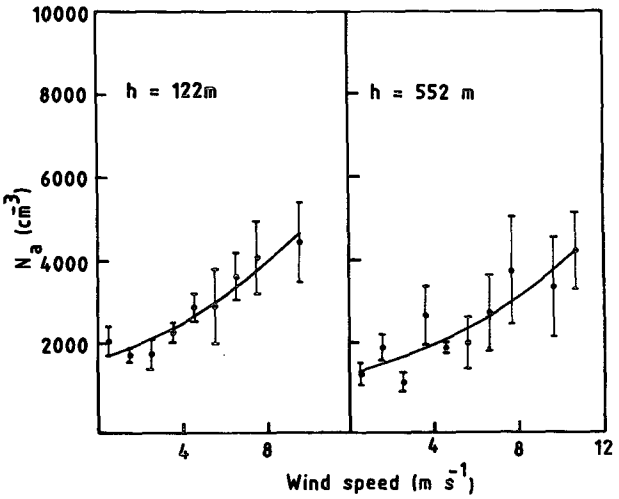


FIG. 3. Variation of aerosol number densities at two typical fixed altitudes, 122 and 552 m, with the wind speed.

aerosols remain the same. The amount of its contribution will vary according to the wind speed (Exton et al. 1985). So the aerosol profiles obtained in different seasons are treated together to study the effect of wind speed. Figure 2 shows the altitude variation of the correlation coefficient $R$ between $U$ and $N_a$ at different altitudes. While each point on this curve represents the value of $R$ between $U$ and $N_a$(h), the associated horizontal line indicates the error of the estimated correlation (Fisher 1970). The 95% level of significance is indicated by a dashed vertical line. As the sea breeze is maximum around 1500 IST, this wind speed is taken as an index to represent the wind effect. The correlations are relatively high in the lower altitudes, indicating that the effect of wind speed on $N_a$ is more significant at lower altitudes. It may be noted that even though the correlation coefficients in the altitude region 300–400 m are smaller than those in the altitude region below, they are still above the 95% level of significance. Thus, in the altitude region 50–1100 m, the aerosol number density $N_a$ is well correlated with the wind speed, having significance level greater than 95%.

To find out the functional dependence of aerosols on the wind speed, we have considered the wind speed values $U$ at 1500 IST, at which the sea-breeze activity is maximum, as pointed out earlier. As seen from Fig. 2, the values of the estimated correlation coefficients (between $U$ and $N_a$) for different altitudes are significant above the 95% level. To quantify the wind speed dependence, the values of $N_a$ at each altitude are grouped at wind speed intervals of 1 m s$^{-1}$ and then averaged. These are plotted against the mean wind speed of each interval. Such plots for two altitudes 122 and 552 m are presented in Fig. 3. The vertical lines represent the standard error of the mean $\sigma n^{-1/2}$, $\sigma$ being the standard deviation and $n$ the number of values of $N_a$ for each wind speed interval of 1 m s$^{-1}$. These plots indicate a nonlinear relation between $N_a$ and $U$. A nonlinear relationship of the form

$$N_a = N_{a0} e^{bU} \qquad (1)$$

has been used (Exton et al. 1985) to express the aerosol number density at different altitudes. In this equation, $b$ is a constant (for any given altitude) and $N_{a0}$ the aerosol number density at $U = 0$.

Using Eq. (1), the values of $N_{a0}$ and $b$ are evaluated for different altitudes by fixing the best-fit curve on the respective $U$–$N_a$ plots. These values of $N_{a0}$ and $b$, plot-

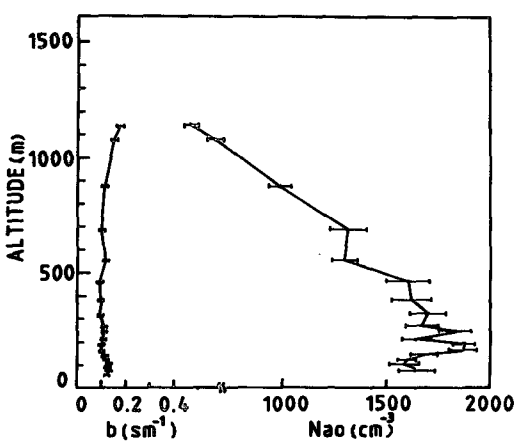


FIG. 4. Altitude variation of $b$ and $N_{a0}$ obtained using the aerosol number density profiles during the period of analysis. The horizontal lines indicate the associated standard error.

ted as a function of altitude, are presented in Fig. 4. The horizontal lines represent the standard error of the coefficients at each altitude. The value of $b$ remains almost a constant throughout the altitude range of 50–1100 m, showing that the wind speed dependence of aerosol number density remains almost the same throughout this altitude. The average value of $b$ comes out to be $0.12 \pm 0.02$ s m$^{-1}$. It will be interesting to compare this value of $b$ with the values reported by other investigators. Most of these studies relate the sea-salt mass loading and wind speed. The value of $b$ ($\approx$0.16 s m$^{-1}$) reported by Woodcock (1953) at 20°N and Lovett (1978) at 50°–60°N compares favorably with the value obtained in the present investigation. Exton et al. (1985) studied the wind speed dependence of aerosol number density at South Uist (56.4°N, 6.1°W) separately for three size ranges, namely, small particles (0.1–0.3 $\mu$m), the large particles (0.3–8 $\mu$m), and the ultralarge particles (8–16 $\mu$m). The average values of $b$ obtained by them for these size ranges were respectively 0.07, 0.13, and 0.24 s m$^{-1}$. When all these size ranges were put together, they obtained a value of 0.16 s m$^{-1}$ for $b$ at a height of 15 m. While Kulkarni et al. (1982) reported a value of 0.27 s m$^{-1}$ over the west coast of India, 1.8 km inland, the value of $b$ obtained by Suzuki and Tsunogai (1988) at Okushiri Island (42.2°N, 139.8°W) in Japan is 0.09 s m$^{-1}$. Hoppel et al. (1990), from their shipborne experiment (20°–40°N) in the Atlantic Ocean, obtained a value close to 0.17 s m$^{-1}$. The value of $b$ obtained in the present investigation compares fairly well with the values quoted above, except that of Kulkarni et al. (1982), who made this study at Tarapur (latitude 19°N) on the west coast of India. They measured the sea-salt concentration at two sites situated, respectively, at 250 m and 1.8 km from the coast, at approximately 1.2 m above the surface. The sea-salt concentration measured at 1.8 km from the coast was used to study the wind speed dependence. They also observed that the measured sea-salt concentration has been depleted by a factor of 2 at 1.8 km inland as compared with that at 250 m off the coast. This could lead to higher values of $b$ as observed by Kulkarni et al. (1982).

Altitude profile of $N_{a0}$ in Fig. 4 represents the altitude (average for the period 1989–90) distribution of aerosol number density in the mixing region adjusted to zero wind speed. The aerosol number density remains almost uniform in the altitude region below 300 m. This is usually referred to as the vertical extent of the well-mixed layer (Sasano 1985; Sasano et al. 1982) or the mixing height. This mixing height is about 100 m higher than the altitude of daytime thermal internal boundary layer (TIBL) observed over this station (Kunhikrishnan et al. 1993). The altitude region above the surface up to the mixing height is the well-mixed layer. Above the well-mixed layer, the aerosol number density first decreases rapidly (called the entrainment or transition layer) and then rather slowly with increase in altitude. It is through this entrainment region, which extends to approximately 200 m above the mixing height, that the mixed layer intrudes into the atmosphere above.

It will be interesting in this context to examine the altitude profile of $N_{a0}$ during the monsoon and nonmonsoon months separately. As the wind direction remains the same during both the seasons, the same relationship between wind speed and $N_a$ can be assumed to hold good for these two seasons. The values of $N_{a0}$ on different days in the monsoon and nonmonsoon months obtained using Eq. (1) are grouped separately and averaged. The horizontal lines represent the standard error. From these two profiles, it can be seen that the shape of the profile, in general, remains the same except for the fact that the mixing height is greater during the monsoon months. This can be attributed to the increase in mechanical mixing caused by the increase in wind shears during the monsoon (Rao 1976). There is a general increase in the value of $N_{a0}$ throughout the altitude range of interest in monsoon months compared to nonmonsoon months. This can be attributed to aerosol sources other than due to wind, being stronger in the monsoon season compared to the other months. These sources (natural) can be vegetation, sulfur cycle, nitrogen cycle, and cultivation dust rise. It may also be noted that during monsoon months the relative humidity is greater than that during the nonmonsoon months. This would result in a change in size index and refractive index. However, the effect of this on the deduced $N_a$ values would be about $\pm$15% as described above. Considering profiles 1 and 2 in Fig. 5, the total content increases by a factor of about 60% from the nonmonsoon to the monsoon period, whereas the aerosol optical depth in Fig. 1 increased by about 120%. This shows that the enhancement in the aerosol optical depth (or the number density) in the monsoon

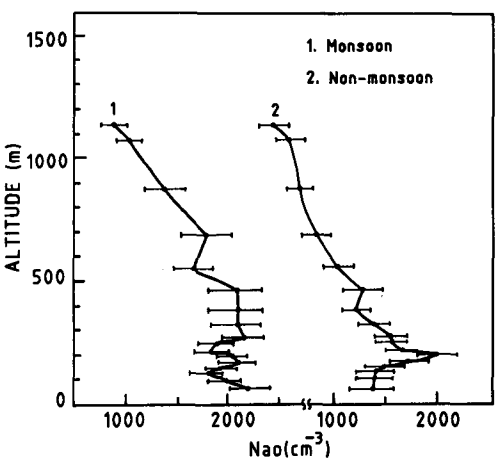


FIG. 5. Altitude variation of the wind-corrected aerosol number density for the monsoon and nonmonsoon months. The horizontal lines indicate the standard error.

season is a result of an enhancement in both the background and wind-contributed components by comparable amounts. The altitude profiles of $N_{a0}$ in Figs. 4 and 5 show a sharp cusp around 200 m. This is more clearly defined in the nonmonsoon months than in the monsoon months. The altitude of this cusp matches fairly well with the altitude of the daytime TIBL (Kunhikrishnan et al. 1993) observed over this station.

## REFERENCES


Delage, Y., 1974: A numerical study of the nocturnal atmospheric boundary layer. *Quart. J. Roy. Meteor. Soc.*, **100,** 351–364.

Exton, H. J., J. Latham, P. M. P., S. J. Perry, and M. H. Smith, 1985: The production and dispersal of marine aerosol. *Quart. J. Roy. Meteor. Soc.*, **111,** 817–837.

Fernald, F. G., B. M. Herman, and J. A. Regan, 1972: Determination of aerosol height distributions by lidar. *J. Appl. Meteor.*, **11,** 482–489.

Fisher, R. A., 1970: *Statistical Methods for Research Workers.* Oliver and Boyed, 194 pp.

Flossmann, A. I., W. D. Hall, and H. R. Pruppacher, 1985: A theoretical study of the wet removal of atmospheric pollutants, Part I: The redistribution of aerosol particles captured through nucleation and impaction scavenging by growing cloud drops. *J. Atmos. Sci.*, **42,** 583–606.

Gathman, S. G., 1983: Optical properties of the marine aerosol as predicted by the Navy aerosol model. *Opt. Eng.*, **22,** 57–62.

Hanel, G., 1976: The properties of atmospheric aerosol particles as functions of relative humidity at thermodynamic equilibrium with the surrounding moist air. *Advances in Geophysics,* Vol. 19, 73–188.

Hidy, G. M., 1984: *Aerosols an Industrial and Environmental Science.* Academic Press Inc., 446 pp.

Hoppel, W. A., J. W. Fitzgerald, G. M. Frick, R. E. Larson, and E. J. Mack, 1990: Aerosol size distributions and optical properties found in the marine boundary layer over the Atlantic Ocean. *J. Geophys. Res.*, **95,** 3659–3686.

Jaenicke, R., 1980: Natural aerosols. *Ann. NY Acad. Sci.*, **338,** 317–322.

——, 1984: Physical aspects of the atmospheric aerosol. *Aerosols and their Climatic Effects,* Eds., H. E. Gerber and A. Deepak, A. Deepak Publishing, 7–34.

Kim, Y. J., H. Sievering, and J. F. Boatman, 1988: Airborne measurements of atmospheric aerosol particles in the lower troposphere over the central United States. *J. Geophys. Res.*, **93,** 12 631–12 644.

Kulkarni, M. R., B. B. Adiga, R. K. Kapoor, and V. V. Skirvaika, 1982: Sea salt in coastal air and its deposition on porcelain insulators. *J. Appl. Meteor.*, **21,** 350–355.

Kunhikrishnan, P. K., K. S. Gupta, R. Ramachandran, J. W. Jeeva Prakash, and K. Narayanan Nair, 1993: Study on thermal internal boundary layer structure over Thumba, India. *Ann. Geophys.*, **11,** 52–60.

Lovett, R. F., 1978: Quantitative measurement of airborne sea-salt in the North Atlantic. *Tellus,* **30,** 358–363.

McClatchey, R. A., R. W. Fenn, J. E. A. Selby, F. E. Volz, and J. S. Garing, 1972: Optical properties of atmosphere. AFCRL-72-0497, AFCRL, Bedford, MA.

Monahan, E. C., C. W. Fairall, K. L. Davidson, and P. J. Boyle, 1983: Observed inter-relations between 10m, winds, ocean whitecaps and marine aerosols. *Quart. J. Roy. Meteor. Soc.*, **109,** 379–392.

Nair, K. N., R. Ramachandran, P. K. Kunhikrishnan, K. Sen Gupta, T. Sunil, K. C. Suma Bai, and S. Muraleedharan Nair, 1993: Dynamics of the atmospheric boundary layer for a tropical seashore station. *13th Int. Congress of Biometeorology,* Calgary, Canada, Int. Soc. Biometeorol.

Parameswaran, K., 1988: Water vapour in the atmosphere: An empirical model for four selected Indian Stations. SPL:SR:003:88, Space Physics Laboratory, Vikram Sarabhai Space Centre, Trivandrum, India, 22 pp.

——, and G. Vijayakumar, 1993: A comparison of aerosol size distributions obtained from bistatic lidar and low-pressure impactor experiments at a coastal station. *Ind. J. Rad. Space Phys.*, **22,** 42–49.

——, K. O. Rose, and B. V. Krishna Murthy, 1984: Aerosol characteristics from bistatic lidar observations. *J. Geophys. Res.*, **89,** 2541–2552.

Park, P. M., M. H. Smith, and H. J. Exton, 1990: The effect of mixing height on maritime aerosol concentrations over the North Atlantic Ocean. *Quart. J. Roy. Meteor. Soc.*, **116,** 461–476.

Prakash, J. W. J., 1993: Atmospheric boundary layer studies at thumba. Ph.D. thesis, University of Kerala, 73 pp.

——, R. Radhika, K. Narayanan Nair, K. Sen Gupta, and P. K. Kunhikrishnan, 1993: On the spectral behaviour of atmospheric boundary layer parameters at Thumba, India. *Quart. J. Roy. Meteor. Soc.*, **119,** 187–197.

Pruppacher, H. R., and J. D. Klett, 1978: *Microphysics of Clouds and Precipitation.* D. Reidal Publishing Co., 714 pp.

Radke, L., M. Eltgroth, and P. Hobbs, 1980: Scavenging of aerosol particles by precipitation. *J. Appl. Meteor.*, **19,** 715–722.

Rao, Y. P., 1976: Southwest monsoon. *Synoptic Meteorology, Meteor. Monogr.,* No. 1/1976, India Meteorological Department.

Sasano, Y., 1985: Observational study on the atmospheric mixed layer and transition layer structures using a Mie lidar. *J. Meteor. Soc. Japan,* **63,** 419–435.

——, A. Shigematsu, H. Shimizu, N. Takeuchi, and M. Okuda, 1982: On the relationship between the aerosol layer height and the mixed layer height determined by laser radar over low-level radiosonde observations. *J. Meteor. Soc. Japan,* **60,** 889–895.

Shettle, E. P., and R. W. Fenn, 1979: Models for the aerosols of the lower atmosphere and the effects of humidity variations on their optical properties. AFGL-TR-79-0214, Environmental Research paper No. 676, 26 pp. [NTIS, ADA 085951]

Suzuki, T., and S. Tsunogai, 1988: Daily variation of aerosols of marine and continental origin in the surface air over a small island, Okushiri in the Japan sea. *Tellus,* **40B,** 42–49.

Toba, Y., 1961: Drop production by bursting of air bubble films on the sea surface (III): Study by use of a wind flume. *Memoirs. Coll. Sci. Univ. Kyoto. Ser. A,* **29,** 313–344.

Woodcock, A. H. 1953: Salt nuclei in marine air as a function of altitude and wind force. *J. Meteor.*, **10,** 362–371.